BJ www.biochemj.org

Biochem. J. (2011) **433**, 197–204 (Printed in Great Britain) doi:10.1042/BJ20101256

online data

The C-terminal basic residues contribute to the chemical- and voltage-dependent activation of TRPA1

Abdul SAMAD*†[1], Lucie SURA*[1], Jan BENEDIKT*, Rudiger ETTRICH†, Babak MINOFAR†, Jan TEISINGER* and Viktorie VLACHOVA*[2]

*Department of Cellular Neurophysiology, Institute of Physiology, Academy of Sciences of the Czech Republic, Videnska 1083, 142 20 Prague 4, Czech Republic, and †Laboratory of Structural Biology, Institute of Systems Biology and Ecology, Academy of Sciences of the Czech Republic, Zamek 136, 373 33 Nove Hrady, Czech Republic

The ankyrin transient receptor potential channel TRPA1 is a non-selective cationic channel that is expressed by sensory neurons, where it can be activated by pungent chemicals, such as AITC (allyl isothiocyanate), cinnamon or allicin, by deep cooling (< 18 °C) or highly depolarizing voltages (>+100 mV). From the cytoplasmic side, this channel can be regulated by negatively charged ligands such as phosphoinositides or inorganic polyphosphates, most likely through an interaction with as yet unidentified positively charged domain(s). In the present study, we mutated 27 basic residues along the C-terminal tail of TRPA1, trying to explore their role in AITC- and voltage-dependent gating. In the proximal part of the C-terminus, the function-affecting mutations were at Lys^{969}, Arg^{975}, Lys^{988} and Lys^{989}. A second significant region was found in the predicted helix, centred around Lys^{1048} and Lys^{1052}, in which single alanine mutations completely abolished AITC- and voltage-dependent activation. In the distal portion of the C-terminus, the charge neutralizations K1092A and R1099A reduced the AITC sensitivity, and, in the latter mutant, increased the voltage-induced steady-state responses. Taken together, our findings identify basic residues in the C-terminus that are strongly involved in TRPA1 voltage and chemical sensitivity, and some of them may represent possible interaction sites for negatively charged molecules that are generally considered to modulate TRPA1.

Key words: C-terminal domain, pleckstrin homology (PH) domain, structure–function relationship, transient receptor potential ankyrin (TRPA), voltage-dependent gating.

INTRODUCTION

The TRPA1 [TRP (transient receptor potential) ankyrin 1] channel is an important constituent of the transduction apparatus through which pro-algesic agents, such as AITC (allyl isothiocyanate), various products of oxidative stress, deep cooling or mechanical stimuli depolarize sensory nerve endings to elicit pain. In addition to a range of pungent chemicals that either bind to (e.g. cannabinoids, icilin, eugenol, carvacrol and thymol) or covalently interact with (e.g. cinnamaldehyde and acrolein) TRPA1, this polymodal non-selective cation channel can also be activated by highly depolarizing voltages (>+100 mV) and Ca^{2+} ions that enter through the channel and bind to its N-terminus [1–11]. Depending on the permeating Ca^{2+}, TRPA1 dynamically controls its own critical properties such as unitary conductance, ion selectivity and open channel probability [12]. An increase in intracellular calcium ($[Ca^{2+}]_i$) not only directly modulates TRPA1 activity, but also recruits cellular Ca^{2+}-dependent signalling cascades which further regulate the channel. Of these, the activation of PLC (phospholipase C), resulting in a decrease in the membrane PIP_2 (phosphatidylinositol 4,5-bisphosphate) is of particular interest, because this signalling lipid may act as an important physiological regulator of TRPA1 in sensory neurons [8,13,14].

The negatively charged ligands, such as phosphoinositides or inorganic polyphosphates, regulate TRPA1 from the cytoplasmic side [9,12,15–20], probably through an interaction with as yet unidentified positively charged domain(s). Based on their analogy to voltage-gated potassium channels [KCNQ, K_{ir} (inwardly rectifying)] and various ion channels of the TRP family [TRPV1 (TRP vanilloid), TRPM4 (TRP melastatin 4), TRPM8], the favourite candidates for the interaction of the TRPA1 channel with negatively charged molecules are the membrane-proximal clusters of positively charged residues on the cytoplasmic C-termini, near to but also further away from the sixth transmembrane domain (for reviews, see [15,21,22]). Such a polybasic region may be able to specifically recognize negatively charged phospholipids, but might also act as a sensor for changes in transmembrane voltage. TRPA1 is a voltage-gated ion channel with an estimated apparent number of gating charges of approx. 0.4 [23]. Compared with voltage-gated potassium channels, the voltage-dependence of TRPA1 is very weak and its putative voltage-sensing domain probably lies outside the conventionally considered fourth transmembrane segment (S4) because it does not contain any charged residues at all. Thus, in addition to the PIP_2-interacting domain(s), the location of the voltage-sensing domain also remains enigmatic and awaits determination.

In the present study, we set out to screen for sites that have the highest probability of being involved in the above processes. We individually altered the charge character of 27 basic residues along the C-terminal tail of human TRPA1 and examined the membrane current responses to voltage, AITC or a combination of the two. We have identified several significant regions within the C-terminus in which positively charged amino acids confer both chemical and voltage sensitivity to TRPA1 channels.

Abbreviations used: AITC, allyl isothiocyanate; HEK-293T cell, human embryonic kidney-293 cell expressing the large T-antigen of SV40 (simian virus 40); PIP_2, phosphatidylinositol 4,5-bisphosphate; TRP, transient receptor potential; TRPA, TRP ankyrin; TRPM, TRP melastatin; TRPV, TRP vanilloid.

[1] These authors contributed equally to this work.

[2] To whom correspondence should be addressed (email vlachova@biomed.cas.cz).

MATERIALS AND METHODS

Expression and constructs of the human TRPA1 channel

HEK-293T cells [human embryonic kidney-293 cells expressing the large T-antigen of SV40 (simian virus 40)] were cultured in OPTI-MEM I medium (Life Technologies) supplemented with 5 % FBS (fetal bovine serum) as described previously [24,25]. Cells were transiently co-transfected with 300–400 ng of cDNA plasmid encoding wild-type or mutant human TRPA1 (wild-type in the pCMV6-XL4 vector, OriGene) and with 300 ng of GFP (green fluorescent protein) plasmid (TaKaRa) per 1.6-mm-diameter dish using the Magnet-assisted Transfection (IBA GmbH) method. Cells were used 24–48 h after transfection. At least two independent transfections were used for each experimental group. The wild-type channel was regularly tested in the same batch as the mutants. The mutants were generated by PCR using the QuikChange® XL Site-Directed Mutagenesis Kit (Stratagene) and confirmed by DNA sequencing (ABI PRISM 3100, Applied Biosystems).

Electrophysiology

Whole-cell membrane currents were recorded by employing an Axopatch 200B amplifier and pCLAMP 10 software (Molecular Devices). Patch electrodes were pulled from a glass tube with a 1.65 mm outer diameter. The tip of the pipette was heat-polished and its resistance was 3–5 MΩ. Series resistance was compensated by at least 70 % in all recordings. Experiments were performed at room temperature (23–25 °C). Only one recording was performed on any one coverslip of cells to ensure that recordings were made from cells not previously exposed to chemical stimuli. Voltage-dependent gating parameters were estimated from steady-state current–voltage (I–V) relationships obtained at the end of 60 or 100 ms voltage steps by fitting the conductance $G = I/(V - V_{rev})$ as a function of the test potential V to the Boltzmann equation:

$$G = [(G_{max} - G_{min})/\{1 + \exp[-zF(V - V_{1/2})/RT]\}] + G_{min}$$

where z is the apparent number of gating charges, $V_{1/2}$ is the half-activation voltage, G_{min} and G_{max} are the minimum and maximum whole-cell conductance, V_{rev} is the reversal potential, and F is Faraday's constant, R is the gas constant, and T is temperature.

A system for rapid superfusion of the cultured cells was used for drug application [26]. The extracellular control solution contained 160 mM NaCl, 2.5 mM KCl, 1 mM $CaCl_2$, 2 mM $MgCl_2$, 10 mM Hepes and 10 mM glucose, adjusted to pH 7.3 and 320 mOsm. In whole-cell patch-clamp experiments, the pipette solution contained 125 mM Cs-gluconate, 15 mM CsCl, 5 mM EGTA, 10 mM Hepes, 0.5 mM $CaCl_2$ and 2 mM MgATP, pH 7.3, 286 mOsm. AITC solution was prepared from a 0.01 M stock solution in water stored at −20 °C. All chemicals were purchased from Sigma–Aldrich.

Statistical analysis

All data were analysed using pCLAMP 10 (Molecular Devices), and curve fitting and statistical analyses were done in SigmaPlot 10 (Systat Software). Statistical significance was determined by Student's t-test or ANOVA; differences were considered significant at $P < 0.05$, if not stated otherwise. For statistical analysis of amplitude data, a logarithmic transformation was used to achieve normal distribution. Conductance–voltage (G–V) relationships were obtained from steady-state whole-cell currents measured at the end of voltage steps from −80 to +200 mV in increments of +20 mV. All data is presented as means ± S.E.M.

RESULTS

Mutations within the C-terminal region identify the residues involved in AITC-induced activation of TRPA1

We individually neutralized all 27 positively charged amino acid residues within the C-terminus of human TRPA1 and characterized the phenotypes of mutants using whole-cell patch-clamp recordings from transiently transfected HEK-293T cells. The primary and putative secondary structure of this region and the residues chosen for mutagenesis are depicted in Figure 1. The C-terminus was predicted to contain two long (H1: Ile^{964}–Lys^{989}, H4: Leu^{1040}–Lys^{1071}) and four short α-helices (H2: Trp^{993}–Val^{998}, H3: Leu^{1016}–Phe^{1022}, H5: Asp^{1089}–Gln^{1095}, H6: Trp^{1103}–Lys^{1111}). We have reported previously that mutations in the predicted inner vestibule of the TRPA1 channel had strong effects on several aspects of channel functioning, including changes in the voltage-dependent activation/deactivation kinetics and a significant increase in the current variance at depolarizing potentials [27]. We then proposed that the pore-forming S6 helix of TRPA1 may extend to the cytoplasmic region so that the proximal portion of the C-terminus, putatively located near the inner mouth of the pore, might directly participate in the regulation of the channel gating or permeation properties. To consider this issue further, we also introduced mutations other than alanine at the most proximal residues: K969E, K969I, K969R, R975E, R975W, K989N and K989E.

The functionality of all mutants was initially established by recording whole-cell currents at a holding potential of −70 mV in response to a supersaturating concentration of AITC (200 μM), applied for 20–30 s in the presence of extracellular Ca^{2+} (1 mM), and by measuring the amplitudes of the currents at the peak (Figure 2A). The period of exposure to AITC was prolonged in those constructs that exhibited slower or incomplete activation kinetics (Figure 2B). As described previously [1,7,9], the AITC-induced responses mediated through wild-type TRPA1 channels were multiphasic with an initial gradually increasing phase followed by a steeper (Ca^{2+}-dependent) secondary phase that occurred 10–20 s after AITC was applied to the cell for the first time. The steep secondary phase of activation was typically followed by an apparent decline in maximal current amplitude ($T_{50} \sim 18$ s), elsewhere referred to as channel inactivation [9,10]. Despite a high degree of cell-to-cell variability in TRPA1 expression and in the magnitudes of AITC-evoked currents within each experimental group, we were able to detect a statistically significant reduction in responsiveness to AITC in ten alanine residue mutants ($P < 0.01$; Figure 2C). Three mutation-affected residues were located in the predicted region of the proximal long canonical α-helix H1: Lys^{969}, Arg^{975} and Lys^{989}. Four residues, Lys^{1046}, Lys^{1048}, Lys^{1052} and Lys^{1071}, were identified within the range of the helix H4 (Figure 1). Mutations K1048A and K1052A did not produce measurable currents in response to AITC at a holding potential of −70 mV and did not exhibit voltage-dependent currents (up to +200 mV in the absence or presence of AITC), thus preventing further evaluation (results not shown). In the distal portion of the C-terminus, a significant reduction in responsiveness to AITC was produced by mutations at the residue Lys^{1009} positioned between helices H2 and H3, at Lys^{1092}, located in the predicted region of the α-helix H5, and at the residue Arg^{1099} between helices H5 and H6.

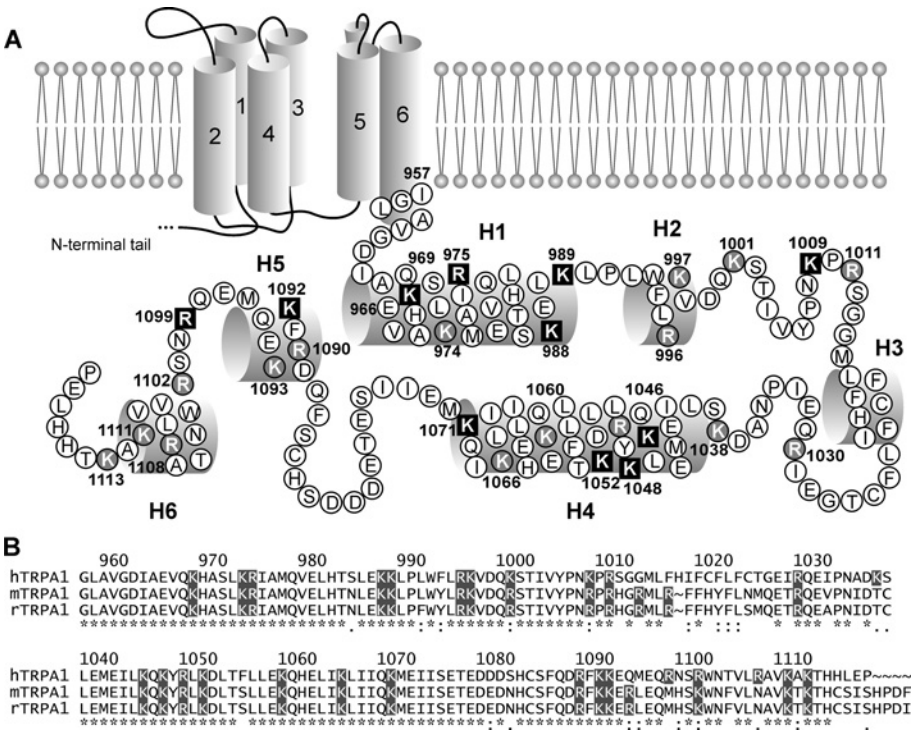

Figure 1 Scanning mutagenesis of the C-terminus of the human TRPA1 channel

(**A**) Putative secondary structure of the human TRPA1 channel subunit with six transmembrane domains and single-letter coded amino acid sequence of the C-terminus. α-helices are shown as cylinders. Positively charged amino acids are indicated (shaded in black or grey). The residues that were found to affect the function of TRPA1 when mutated are indicated by bold white letters on black squares. (**B**) Sequence comparison of the C-terminus of human TRPA1 (hTRPA1; GenBank® accession number NM_007332) with that of mouse (mTRPA1; NM_177781) and rat (rTRPA1; NM_207608) TRPA1. Secondary structure was determined using consensus of four prediction servers (PredictProtein, jPRED, APSSP2 and YASSPP). The structure was assigned if at least three of four servers predict to the residuum the same structure with an expected average accuracy over 80 % or reliability over 5. On the basis of these conditions, the C-terminus is predicted to contain two long and four short helices: Ile^{964}–Lys^{989} (H1), Trp^{993}–Val^{998} (H2), Leu^{1016}–Phe^{1022} (H3), Leu^{1040}–Lys^{1071} (H4), Asp^{1089}–Gln^{1095} (H5) and Trp^{1103}–Lys^{1111} (H6).

The phenotypes of AITC-induced activation of the helix H1 mutants K969A (Figure 2B, panel a) and K969I (Figure 2B, panel b) clearly differed from K969E (Figure 2B, panel c) and from wild-type channels (Figure 2A) in that their responses were smaller and the onset of the secondary phase (if any) was apparently slower. The K969E mutant did not exhibit significant changes in the average amplitude of the AITC-induced currents. In contrast with the wild-type, however, it lacked the first, gradually increasing activation phase (Figure 2B, panel c), indicating that either the gating properties of the channel are altered or permeating Ca^{2+} contributes much faster or more effectively to the potentiation of the response. In helix H1, for mutants K989E (Figure 2B, panel g) and K989N (Figure 2B, panel h), the steep secondary phase only developed upon prolonged (>40 s) application. In K969R (Figure 2B, panel d), R975A (Figure 2B, panel e), K989A (Figure 2B, panel f), K1071A (Figure 2B, panel k) and K1092A (Figure 2B, panel l), the secondary phase of activation was not observed within the ~40 s period of AITC exposure; the responses were small and tended to inactivate upon prolonged AITC stimulation. Notably, R975A exhibited only small, linearly increasing inward currents accompanied by marked increases in current noise, indicating that the AITC-evoked currents arose from a fast opening of ion channels. Mutations R975E and R975W did not produce measurable currents in response to AITC at a holding potential of −70 mV and did not exhibit voltage-dependent currents up to +200 mV (results not shown). Thus in this initial screening we identified ten basic residues that when mutated disrupted channel sensitivity to AITC, indicating that the C-terminus is a critical modulatory domain of TRPA1.

Mapping residues critical for the regulation of TRPA1 by voltage

The voltage-dependent activation properties were assessed in another set of experiments from the steady-state conductances at various test potentials using a voltage step protocol from −80 mV up to +200 mV in steps of +20 mV, measured first in the extracellular control solution, and, in those mutants with altered AITC or voltage sensitivity, also in the maintained presence of 200 μM AITC. In these experiments, we took care to fully activate the channels and thus the voltage step protocol was applied immediately at the peak amplitude of the first AITC response (Figure 3A). By measuring the maximum steady-state outward currents at +200 mV recorded in extracellular control solution, we detected significant changes in eight alanine residue substitutions at $P < 0.01$ (Figure 3B). Of these, Lys^{969} (Figure 3A, panels b–e), Arg^{975} (Figure 3A, panel f) and Lys^{989} (Figure 3A, panels h–j) appeared to be of major importance for the voltage-dependent activation of TRPA1, since mutations at these sites exhibited phenotypes that were kinetically clearly different from the wild-type. The voltage-induced currents mediated by K1009A and K1071A, although significantly smaller in amplitude, were kinetically indistinguishable from the wild-type channel. In contrast, the outward currents mediated through R1099A were larger than those in wild-type TRPA1 (results not shown).

The charge-reversing mutation K969E (Figures 3C and 3D) had strong effects on three important parameters of voltage-dependent gating: (i) saturation followed by a decrease in the maximum outward conductance at voltages higher than approx. +140 mV; (ii) increasing the current variance at strongly (>+100 mV)

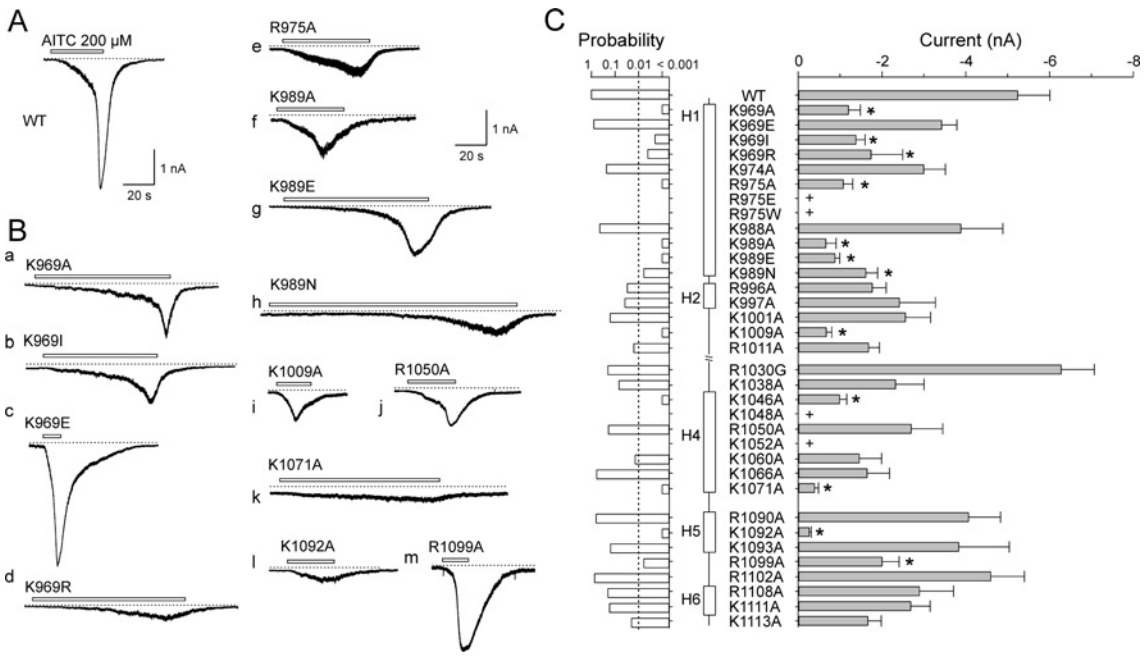

Figure 2 Screen of the C-terminus of human TRPA1 for AITC sensitivity

(**A** and **B**) Examples of whole-cell currents elicited by 200 μM AITC from HEK-293T cells transiently transfected with (**A**) wild-type (WT) TRPA1 or (**B**, panels a–m) mutant TRPA1 channels that exhibited the most prominent phenotypic changes. Broken lines indicate zero current level. Horizontal bars above each record indicate the duration of AITC application. Holding potential −70 mV. (**C**) Summary of scanning mutagenesis results comparing sensitivity to AITC. The right histogram shows mean whole-cell currents evoked by 200 μM AITC at −70 mV measured at the peak for each construct. Each bar is the means ± S.E.M. of at least six independent cells. The left histogram represents the probabilities obtained from the *t* tests that were performed in order to determine if there was a significant difference between the responses of the wild-type and the individual mutants. The level of significance is indicated with a broken vertical line in the left probability histogram. Statistical significance ($P < 0.01$) is indicated with asterisks in the right current histogram. The plus signs indicate positions where mutations resulted in constructs lacking functional expression in HEK-293T cells. The predicted secondary structure is indicated in the middle as vertical thick bars (α-helices H1, H2, H4–H6).

depolarizing potentials; and (iii) slowing the decay kinetics of tail currents that arise upon repolarization to −70 mV from various test potentials. This phenotype was particularly remarkable, because a similar pattern of responses at positive potentials was previously reported for wild-type mouse TRPA1 (see the Discussion) [18,28].

Under control conditions, mutations R975A, K989A and K989E exhibited higher outward current amplitudes (Figure 3B) and a stronger outward rectification than wild-type TRPA1 (rectification ratios G_{+180mV}/G_{-60mV}; 37.5 ± 2.2 for R975A, 18.8 ± 2.8 for K989A and 28 ± 13 for K989E compared with 11.1 ± 3.5 for wild-type; $n = 3$–6) (Figures 4A and 4B). Kinetically clearly different phenotypes were obtained with R975A, K988A, K989A, K989E and K989N, which exhibited prominent changes in the onset kinetics of their voltage-induced responses (Figure 3A, panels f–j). Specifically, in R975A (Figure 3A, panel f), the onset of the voltage-induced outward currents was instantaneous upon depolarization and only very small tail currents were inwardly directed upon repolarization from +200 mV to −70 mV, indicating that the mutant has very fast gating kinetics or that the inward movement of cations through the conduction pathway of the channel is blocked at negative membrane potentials. Compared with wild-type TRPA1 (53.1 ± 4.6 ms; $n = 5$), the activation time constant for outward currents measured at +200 mV, obtained by fitting a monoexponential function to the current traces (τ_{on}), was much faster in K988A (23.5 ± 2.2 ms; $n = 4$). Also, in K989A, τ_{on} was 25.9 ± 4.2 ms ($n = 3$), and this value was not significantly different from that in K989E (25.1 ± 3.6 ms; $n = 5$; $P = 0.884$) or K989N (32.7 ± 0.4 ms; $n = 3$; $P = 0.49$), implying that the functional changes caused by mutations at Lys^{989} are likely to be steric rather than affected by charge. In the control extracellular solution (Figure 4D, panels a and b), the open probabilities for wild-type TRPA1 were apparently below 0.5 so that values for the voltage for half-maximal activation (V_{50}) could not be derived from steady-state currents [4,29]. In contrast, the conductance–voltage (*G–V)* relationships were shifted toward less depolarizing potentials in K969A ($V_{50} = 107.2 \pm 7.5$ mV; $n = 4$), R975A (106 ± 14 mV; $n = 7$) and K989A (87.2 ± 16 mV; $n = 3$), indicating an enhanced voltage-dependent activity at more physiological potentials.

Conductance–voltage relationships obtained in the presence of AITC

Voltage is a weak partial activator of TRPA1 that synergizes with other stimuli such as AITC or Ca^{2+} and regulates channel opening in an allosteric manner [4,11,23,29]. To further characterize the sensitivity of voltage-induced activation for all mutants with altered phenotypes, we measured the voltage-dependent component of gating from the conductance–voltage (*G–V)* relationships obtained in the presence of 200 μM AITC, compared at positive against negative membrane potentials (G_{+180}/G_{-60mV}). The *G-V* relationships were virtually voltage-independent in wild-type TRPA1 (1.3 ± 0,16; $n = 6$) and in K988A (1.1 ± 0.1; $n = 3$; Figures 4C and 4D, panels c and d). In contrast, the percentage of the voltage-dependent component of AITC-induced gating (G_{+180}/G_{-60mV}) was strongly ($P < 0.01$) increased in R975A (3.40 ± 0.68; $n = 3$), K989A (7.7 ± 2.0; $n = 3$), K989E (8.6 ± 2.0; $n = 6$) and K989N (3.45 ± 0.47; $n = 6$) (Figures 4B and 4C, and 4D, panels c and d). Similarly to what was observed in control extracellular solution (Figure 3D), K969E

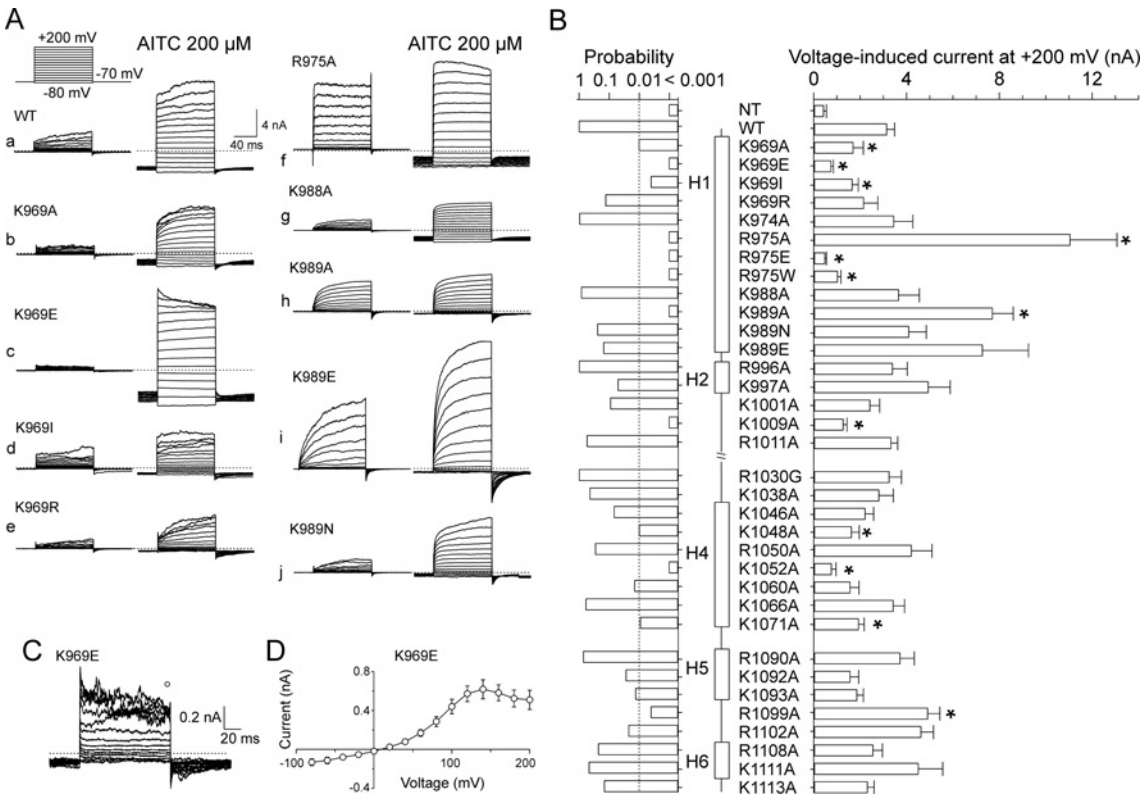

Figure 3 Voltage-dependent gating of TRPA1 mutants

(**A**) Representative current traces in response to the indicated voltage step protocol (holding potential, −70 mV; voltage steps from −80 mV to +200 mV; increment +20 mV) recorded in control extracellular solution (left) and in the presence of 200 μM AITC (right). (**B**) Summary of mutagenesis results. Average steady-state whole-cell currents induced by voltage (+200 mV). Each bar is the means ± S.E.M. of at least six independent cells. The predicted secondary structure is indicated in the middle as vertical thick bars (α-helices H1, H2, H4–H6). The left histogram represents the probabilities obtained from the *t* tests that compared the steady-state current amplitudes of the individual mutants with the wild-type (WT). The level of significance is indicated with a broken vertical line in the left probability histogram. Statistical significance ($P < 0.01$) is indicated with asterisks in the right current histogram. (**C**) Representative whole-cell currents evoked by the voltage protocol (shown in **A**) applied in control extracellular solution, recorded in the K969E mutant. (**D**) Averaged voltage–current relationship constructed from responses obtained from eight independent recordings such as shown in (**C**), measured at the end of the pulses (indicated above the records in **C**). Results are means ± S.E.M. NT, non-transfected HEK-293T cells.

exhibited saturation followed by a decrease in the maximum outward conductance at voltages higher than approx. +120–140 mV (Figure 4D, panel d), which might indicate that the negative charge at this position interferes with the outward permeation of cations or that the mutation caused a defect in the voltage-dependent gating (see Discussion for additional possibilities).

Taken together, these data point to a possible differential role for Lys^{969}, Arg^{975}, Lys^{988}, Lys^{989}, Lys^{1009}, Lys^{1071} and Arg^{1099} in the voltage-dependent modulation of TRPA1. Except for Lys^{988}, mutations at these residues also altered the AITC sensitivity (Figure 2C). Moreover, the potentiating effects of mutations at Lys^{989} were independent of the charge, suggesting that they might arise from the removal of the long lysine side chain. Thus the changes in voltage-dependent activation in this mutant are probably due to alterations in channel gating rather than a direct effect on the putative voltage-transduction mechanism.

DISCUSSION

In the present study, by performing the systemic neutralization of 27 positively charged residues within the C-terminal region of human TRPA1, we identified a limited number of residues that appear to be important to the allosteric regulation of the channel by both chemical and voltage stimuli (Lys^{969}, Arg^{975}, Lys^{989}, Lys^{1009}, Lys^{1046}, Lys^{1071}, Lys^{1092} and Arg^{1099}). These residues are therefore most likely to be involved in the transduction of the activation signals to the gate rather than being the primary sites for either AITC binding or voltage sensing. In addition, we characterized three charge-neutralizing 'gain-of-function' mutants (R975A, K988A and K989A) which exhibited higher sensitivity to depolarizing voltages, indicating that these residues may be directly involved in the voltage-dependent modulation of TRPA1.

Functional role of the most proximal helix of the C-terminus

Site-directed mutagenesis studies have previously shown that AITC activates TRPA1 by covalently reacting with cysteine residues in the cytoplasmic N-terminus of the channel [4,5]. The C-terminal basic residues, mutations of which significantly reduced responsiveness to AITC, thus may be part of a transduction region which transmits AITC signal from the N-terminus to the gate. Those residues that are structurally proximal to the sixth transmembrane domain may directly participate in channel gating or contribute to the formation of the permeation pathway. Also, the possibility of indirect electrostatic effects (such as interaction with some negatively charged ligands) cannot be excluded for any of the affected residues.

Mutation of Lys^{969} to glutamate produced a channel with a very distinctive phenotype. This mutant did not exhibit

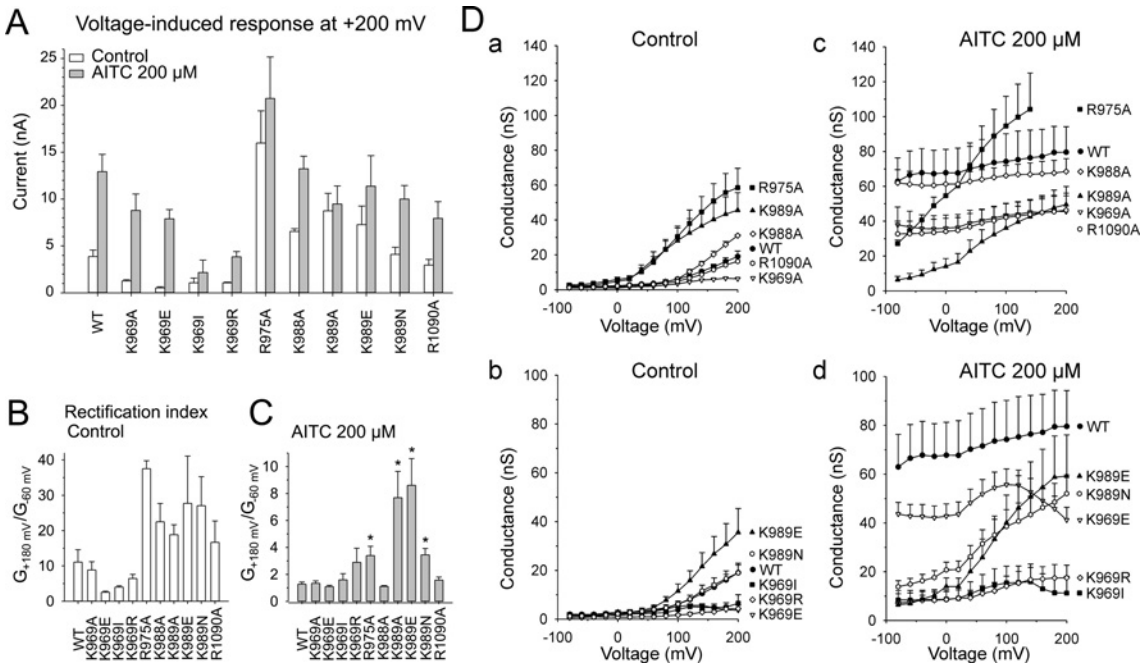

Figure 4 Effects of mutations on the AITC-modulation of voltage-dependent gating

(**A**) Effects of 200 μM AITC on maximal voltage-induced outward currents of TRPA1 mutants. Steady-state currents evoked by +200 mV measured in the absence (open bars) and presence (grey bars) of 200 μM AITC. (**B**) Outward rectification properties (G_{+180mV}/G_{-60mV}) reflecting the effects of mutations on voltage-dependent gating. (**C**) Summary of the voltage-dependent component of AITC-induced gating (G_{+180mV}/G_{-60mV}). *$P < 0.01$ compared with wild-type (WT). (**D**) Summary of whole-cell conductances obtained in the absence (left graphs) and presence of 200 μM AITC (right graphs) for wild-type and for the indicated constructs. Under control conditions, the wild-type channels and some mutants did not reach half-maximal activation at voltages up to +200 mV. Each plot shows the means $\pm$ SEM; $n = 3$–8.

significant changes in the average amplitude of the AITC-induced currents but it lacked the first, gradually increasing activation phase (Figure 2B, panel c, and Supplementary Figure S1A at http://www.BiochemJ.org/bj/433/bj4330197add.htm). This might indicate that either the gating properties of the channel are altered and/or permeating Ca^{2+} contributes much faster or more effectively to the potentiation of the responses. In order to distinguish further if the mutation-induced changes in the functionality of K969E stem from changes in gating or from alterations in the ion permeation or selectivity properties, we measured the Ca^{2+} permeability relative to Cs^+ (Supplementary Figure S1B). We found that the K969E mutation yielded channels with unchanged permeability to Ca^{2+} ($P_{Ca}/P_{Cs} = 3.0 \pm 0.2$; $n = 7$, compared with 3.4 ± 0.3 for wild-type; $n = 6$; $P < 0.05$), which indicates that the K969E mutation does not affect the ion permeation process and most likely does not indirectly influence Ca^{2+}-dependent gating at negative membrane potentials. Such a conclusion is strengthened further by our previously reported data showing that Glu^{966}, which is located approximately one helix turn downward from Lys^{969}, is probably poorly situated within the transmembrane electric field and neither sterically nor electrostatically contributes to forming the ion conduction pathway [27]. The charge-reversing mutation K969E had strong effects on voltage-dependent activation; at depolarizing potentials higher than approx. +140 mV, the maximum outward currents were decreased, whereas the current variance increased (Figures 3C and 3D). In addition, various mutations at Lys^{969} revealed that the channel does not well tolerate alanine, isoleucine or arginine at this position, which might be an additional indication that Lys^{969} indeed plays a structural role in gating. Interestingly, a similar pattern of decay of responses at positive membrane potentials was previously reported for CHO (Chinese-hamster ovary) cells expressing wild-type mouse TRPA1 and has been attributed to channel inactivation [18] or to 'a time-dependent increase in open probability, overlaid by a block of the ion channels by some unknown mechanism' [28]. Moreover, in the latter study, very similar voltage-dependent properties were seen with H_2O_2 and AITC-evoked currents in Ca^{2+}-free solution, indicating that Ca^{2+}-dependent inactivation of TRPA1 is not the likely mechanism.

Possible involvement of the C-terminus in voltage-dependent activation

Mutations at Arg^{975}, Lys^{988} and Lys^{989} directly affected voltage-dependent gating under control conditions, suggesting that these residues may be part of a voltage sensor. In contrast with voltage-gated potassium channels, the voltage sensitivity of TRPA1 is very weak and there is virtually nothing known about what parts of the channel are involved in voltage sensing [30]. Therefore it is not clear whether these three residues might be included in the electric field of the membrane. The robust steady-state outward rectification and leftward shift in the voltage-dependent activation observed in R975A and K989A (and, to a lesser extent, also in K988A) may be the consequence of the fact that both residues are situated on the same (more hydrophobic) side of the first proximal helix: the neutralization of either of these residues could similarly reduce the overall electrostatic effect.

The saturating concentration of agonist has been shown to reveal the voltage-independent component of gating in TRPA1-related TRPV1 and TRPM8 channels [31]. By using a voltage stimulus in combination with a supramaximal concentration of AITC (200 μM), we hoped to distinguish

between the voltage-dependent and voltage-independent modes of TRPA1 activation to better understand the specific role of the identified residues. In thermosensitive TRP channels, chemical and thermal stimuli interact allosterically through independent molecular mechanisms. In TRPV1, vanilloids interact at intracellular/intramembranous regions in and adjacent to S3 and S4 [32,33]; a small region of the proximal part of the C-terminal domain renders the TRPV1 channel heat-sensitive and this region is transplantable into the cold-sensitive TRPM8 channel, whose voltage-induced responses become potentiated by heat [34]. A strong piece of evidence in favour of mechanistically distinguishable activation mechanisms was also recently presented for TRPV1 and TRPV3, in which agonist- and temperature-induced activations are separable from other activation mechanisms [35–38]. However, the intrinsic mechanism by which polymodal TRP channels are gated by voltage is much less clear. In another TRPA1-related channel, TRPV4, the main agonist-activated intracellular gate works independently of the voltage-dependent gating mechanism [39]. As pointed out by the authors (see Discussion in [39]), several possible candidates for the voltage-gating mechanism have to be generally considered for the family of TRP-related cation channels: one of the possible models relies on a filter gating mechanism, which is based on the evidence that filter region gating underlies TRPV1-channel activation [40,41]. In this case, the principle role for voltage might be the control of the direction of the driving force. This seems unlikely in TRPA1 because the channel becomes voltage-independent in the presence of a supersaturating concentration of AITC (Figure 4D). Another model of the voltage-dependent gating mechanism relies on direct voltage-dependent closure of the intracellular gate. Given that the activation rates upon depolarization were substantially accelerated in R975A, K988A and K989A, we cannot dismiss the possibility that these residues could be directly involved in the voltage-dependent gating.

CONCLUSIONS

In the present study, we identified the residues within the putative C-terminal tail of the human TRPA1 channel that, when mutated, affect its AITC and/or voltage sensitivity. In most cases, the reduced magnitudes of the responses to AITC or voltage were not due to reduced expression levels or plasma membrane targeting, since: (i) simultaneous application of both stimuli revealed considerable differences in the relative cross-sensitization capacity among the mutants; (ii) several mutants were less specifically responsive to AITC or voltage, i.e. their current–voltage relationships were qualitatively different from that in the wild-type channel or their AITC-induced inward currents lacked the steep secondary phase of activation; and, moreover, (iii) although there was a substantial overlap between the AITC- and voltage-deficient mutants, several of them exhibited significantly opposite effects on these two modalities (e.g. R975A, R989A and R1099A; compare Figure 2C with Figure 3B). Although further mutagenesis is required to determine the exact nature of the identified residues, our findings provide strong support for the role of multiple basic residues in the re-cognition of chemical and voltage stimuli and indicate that the C-terminus is a critical modulatory domain for TRPA1 activation.

AUTHOR CONTRIBUTION

Lucie Sura planned, performed and analysed experiments. Jan Benedikt performed experiments. Abdul Samad, Rudiger Ettrich and Babak Minofar performed and analysed experiments. Jan Teisinger planned and performed experiments. Viktorie Vlachova planned and analysed experiments, and wrote the paper.

FUNDING

This work was supported by the Czech Science Foundation [grant numbers 305/06/0319, 301/10/1159], the Research Project Fund of the ASCR (Academy of Sciences of the Czech Republic) [grant numbers AV0Z50110509, AV0Z60870520, IAA 600110701], and by the Ministry of Education, Youth and Sports of the Czech Republic [grant numbers 1M0517, LC06010, MSM6007665808, LC554].

REFERENCES

1 Story, G. M., Peier, A. M., Reeve, A. J., Eid, S. R., Mosbacher, J., Hricik, T. R., Earley, T. J., Hergarden, A. C., Andersson, D. A., Hwang, S. W. et al. (2003) ANKTM1, a TRP-like channel expressed in nociceptive neurons, is activated by cold temperatures. Cell **112**, 819–829
2 Zhang, X. F., Chen, J., Faltynek, C. R., Moreland, R. B. and Neelands, T. R. (2008) Transient receptor potential A1 mediates an osmotically activated ion channel. Eur. J. Neurosci. **27**, 605–611
3 Sawada, Y., Hosokawa, H., Hori, A., Matsumura, K. and Kobayashi, S. (2007) Cold sensitivity of recombinant TRPA1 channels. Brain Res. **1160**, 39–46
4 Macpherson, L. J., Dubin, A. E., Evans, M. J., Marr, F., Schultz, P. G., Cravatt, B. F. and Patapoutian, A. (2007) Noxious compounds activate TRPA1 ion channels through covalent modification of cysteines. Nature **445**, 541–545
5 Hinman, A., Chuang, H. H., Bautista, D. M. and Julius, D. (2006) TRP channel activation by reversible covalent modification. Proc. Natl. Acad. Sci. U.S.A. **103**, 19564–19568
6 Cavanaugh, E. J., Simkin, D. and Kim, D. (2008) Activation of transient receptor potential A1 channels by mustard oil, tetrahydrocannabinol and Ca^{2+} reveals different functional channel states. Neuroscience **154**, 1467–1476
7 Garcia-Anoveros, J. and Nagata, K. (2007) TRPA1. Handb. Exp. Pharmacol. **179**, 347–362
8 Bautista, D. M., Jordt, S. E., Nikai, T., Tsuruda, P. R., Read, A. J., Poblete, J., Yamoah, E. N., Basbaum, A. I. and Julius, D. (2006) TRPA1 mediates the inflammatory actions of environmental irritants and proalgesic agents. Cell **124**, 1269–1282
9 Nagata, K., Duggan, A., Kumar, G. and Garcia-Anoveros, J. (2005) Nociceptor and hair cell transducer properties of TRPA1, a channel for pain and hearing. J. Neurosci. **25**, 4052–4061
10 Doerner, J. F., Gisselmann, G., Hatt, H. and Wetzel, C. H. (2007) Transient receptor potential channel A1 is directly gated by calcium ions. J. Biol. Chem. **282**, 13180–13189
11 Zurborg, S., Yurgionas, B., Jira, J. A., Caspani, O. and Heppenstall, P. A. (2007) Direct activation of the ion channel TRPA1 by Ca^{2+}. Nat. Neurosci. **10**, 277–279
12 Wang, Y. Y., Chang, R. B., Waters, H. N., McKemy, D. D. and Liman, E. R. (2008) The nociceptor ion channel TRPA1 is potentiated and inactivated by permeating calcium ions. J. Biol. Chem. **283**, 32691–32703
13 Bandell, M., Story, G. M., Hwang, S. W., Viswanath, V., Eid, S. R., Petrus, M. J., Earley, T. J. and Patapoutian, A. (2004) Noxious cold ion channel TRPA1 is activated by pungent compounds and bradykinin. Neuron **41**, 849–857
14 Wang, S., Dai, Y., Fukuoka, T., Yamanaka, H., Kobayashi, K., Obata, K., Cui, X., Tominaga, M. and Noguchi, K. (2008) Phospholipase C and protein kinase A mediate bradykinin sensitization of TRPA1: a molecular mechanism of inflammatory pain. Brain **131**, 1241–1251
15 Nilius, B., Owsianik, G. and Voets, T. (2008) Transient receptor potential channels meet phosphoinositides. EMBO J. **27**, 2809–2816
16 Corey, D. P., Garcia-Anoveros, J., Holt, J. R., Kwan, K. Y., Lin, S. Y., Vollrath, M. A., Amalfitano, A., Cheung, E. L., Derfler, B. H., Duggan, A. et al. (2004) TRPA1 is a candidate for the mechanosensitive transduction channel of vertebrate hair cells. Nature **432**, 723–730
17 Hirono, M., Denis, C. S., Richardson, G. P. and Gillespie, P. G. (2004) Hair cells require phosphatidylinositol 4,5-bisphosphate for mechanical transduction and adaptation. Neuron **44**, 309–320
18 Karashima, Y., Prenen, J., Meseguer, V., Owsianik, G., Voets, T. and Nilius, B. (2008) Modulation of the transient receptor potential channel TRPA1 by phosphatidylinositol 4,5-biphosphate manipulators. Pflugers Arch. **457**, 77–89
19 Akopian, A. N., Ruparel, N. B., Jeske, N. A. and Hargreaves, K. M. (2007) Transient receptor potential TRPA1 channel desensitization in sensory neurons is agonist dependent and regulated by TRPV1-directed internalization. J. Physiol. **583**, 175–193
20 Kim, D., Cavanaugh, E. and Simkin, D. (2008) Inhibition of transient receptor potential A1 by phosphatidylinositol-4,5-bisphosphate. Am. J. Physiol. Cell Physiol. **295**, C92–C99
21 Rohacs, T. (2009) Phosphoinositide regulation of non-canonical transient receptor potential channels. Cell Calcium **45**, 554–565

22 Suh, B. C. and Hille, B. (2008) PIP_2 is a necessary cofactor for ion channel function: how and why? Annu. Rev. Biophys. **37**, 175–195
23 Karashima, Y., Talavera, K., Everaerts, W., Janssens, A., Kwan, K. Y., Vennekens, R., Nilius, B. and Voets, T. (2009) TRPA1 acts as a cold sensor *in vitro* and *in vivo*. Proc. Natl. Acad. Sci. U.S.A. **106**, 1273–1278
24 Susankova, K., Ettrich, R., Vyklicky, L., Teisinger, J. and Vlachova, V. (2007) Contribution of the putative inner-pore region to the gating of the transient receptor potential vanilloid subtype 1 channel (TRPV1). J. Neurosci. **27**, 7578–7585
25 Vlachova, V., Teisinger, J., Suánková, K., Lyfenko, A., Ettrich, R. and Vyklicky, L. (2003) Functional role of C-terminal cytoplasmic tail of rat vanilloid receptor 1. J. Neurosci. **23**, 1340–1350
26 Dittert, I., Benedikt, J., Vyklicky, L., Zimmermann, K., Reeh, P. W. and Vlachova, V. (2006) Improved superfusion technique for rapid cooling or heating of cultured cells under patch-clamp conditions. J. Neurosci. Methods **151**, 178–185
27 Benedikt, J., Samad, A., Ettrich, R., Teisinger, J. and Vlachova, V. (2009) Essential role for the putative S6 inner pore region in the activation gating of the human TRPA1 channel. Biochim. Biophys. Acta **1793**, 1279–1288
28 Andersson, D. A., Gentry, C., Moss, S. and Bevan, S. (2008) Transient receptor potential A1 is a sensory receptor for multiple products of oxidative stress. J. Neurosci. **28**, 2485–2494
29 Karashima, Y., Damann, N., Prenen, J., Talavera, K., Segal, A., Voets, T. and Nilius, B. (2007) Bimodal action of menthol on the transient receptor potential channel TRPA1. J. Neurosci. **27**, 9874–9884
30 Latorre, R., Zaelzer, C. and Brauchi, S. (2009) Structure-functional intimacies of transient receptor potential channels. Q. Rev. Biophys. **42**, 201–246
31 Matta, J. A. and Ahern, G. P. (2007) Voltage is a partial activator of rat thermosensitive TRP channels. J. Physiol. **585**, 469–482
32 Jordt, S. E. and Julius, D. (2002) Molecular basis for species-specific sensitivity to "hot" chili peppers. Cell **108**, 421–430
33 Gavva, N. R., Klionsky, L., Qu, Y., Shi, L., Tamir, R., Edenson, S., Zhang, T. J., Viswanadhan, V. N., Toth, A., Pearce, L. V. et al. (2004) Molecular determinants of vanilloid sensitivity in TRPV1. J. Biol. Chem. **279**, 20283–20295
34 Brauchi, S., Orta, G., Mascayano, C., Salazar, M., Raddatz, N., Urbina, H., Rosenmann, E., Gonzalez-Nilo, F. and Latorre, R. (2007) Dissection of the components for PIP_2 activation and thermosensation in TRP channels. Proc. Natl. Acad. Sci. U.S.A. **104**, 10246–10251
35 Hu, H., Grandl, J., Bandell, M., Petrus, M. and Patapoutian, A. (2009) Two amino acid residues determine 2-APB sensitivity of the ion channels TRPV3 and TRPV4. Proc. Natl. Acad. Sci. U.S.A. **106**, 1626–1631
36 Grandl, J., Hu, H., Bandell, M., Bursulaya, B., Schmidt, M., Petrus, M. and Patapoutian, A. (2008) Pore region of TRPV3 ion channel is specifically required for heat activation. Nat. Neurosci. **11**, 1007–1013
37 Yang, F., Cui, Y., Wang, K. and Zheng, J. (2010) Thermosensitive TRP channel pore turret is part of the temperature activation pathway. Proc. Natl. Acad. Sci. U.S.A. **107**, 7083–7088
38 Grandl, J., Kim, S. E., Uzzell, V., Bursulaya, B., Petrus, M., Bandell, M. and Patapoutian, A. (2010) Temperature-induced opening of TRPV1 ion channel is stabilized by the pore domain. Nat. Neurosci. **13**, 708–714
39 Loukin, S., Su, Z., Zhou, X. and Kung, C. (2010) Forward-genetic analysis reveals multiple gating mechanisms of Trpv4. J. Biol. Chem. **285**, 19884–19890
40 Myers, B. R., Bohlen, C. J. and Julius, D. (2008) A yeast genetic screen reveals a critical role for the pore helix domain in TRP channel gating. Neuron **58**, 362–373
41 Ryu, S., Liu, B., Yao, J., Fu, Q. and Qin, F. (2007) Uncoupling proton activation of vanilloid receptor TRPV1. J. Neurosci. **27**, 12797–12807

Received 10 August 2010/28 September 2010; accepted 14 October 2010
Published as BJ Immediate Publication 14 October 2010, doi:10.1042/BJ20101256

Biochem. J. (2011) **433**, 197–204 (Printed in Great Britain) doi:10.1042/BJ20101256

online data

SUPPLEMENTARY ONLINE DATA

The C-terminal basic residues contribute to the chemical and voltage-dependent activation of TRPA1

Abdul SAMAD*†[1], Lucie SURA*[1], Jan BENEDIKT*, Rudiger ETTRICH†, Babak MINOFAR†, Jan TEISINGER* and Viktorie VLACHOVA*[2]

*Department of Cellular Neurophysiology, Institute of Physiology, Academy of Sciences of the Czech Republic, Videnska 1083, 142 20 Prague 4, Czech Republic, and †Laboratory of Structural Biology, Institute of Systems Biology and Ecology, Academy of Sciences of the Czech Republic, Zamek 136, 373 33 Nove Hrady, Czech Republic

See the pages that follow for Supplementary Figure S1

[1] These authors contributed equally to this work.
[2] To whom correspondence should be addressed (email vlachova@biomed.cas.cz).

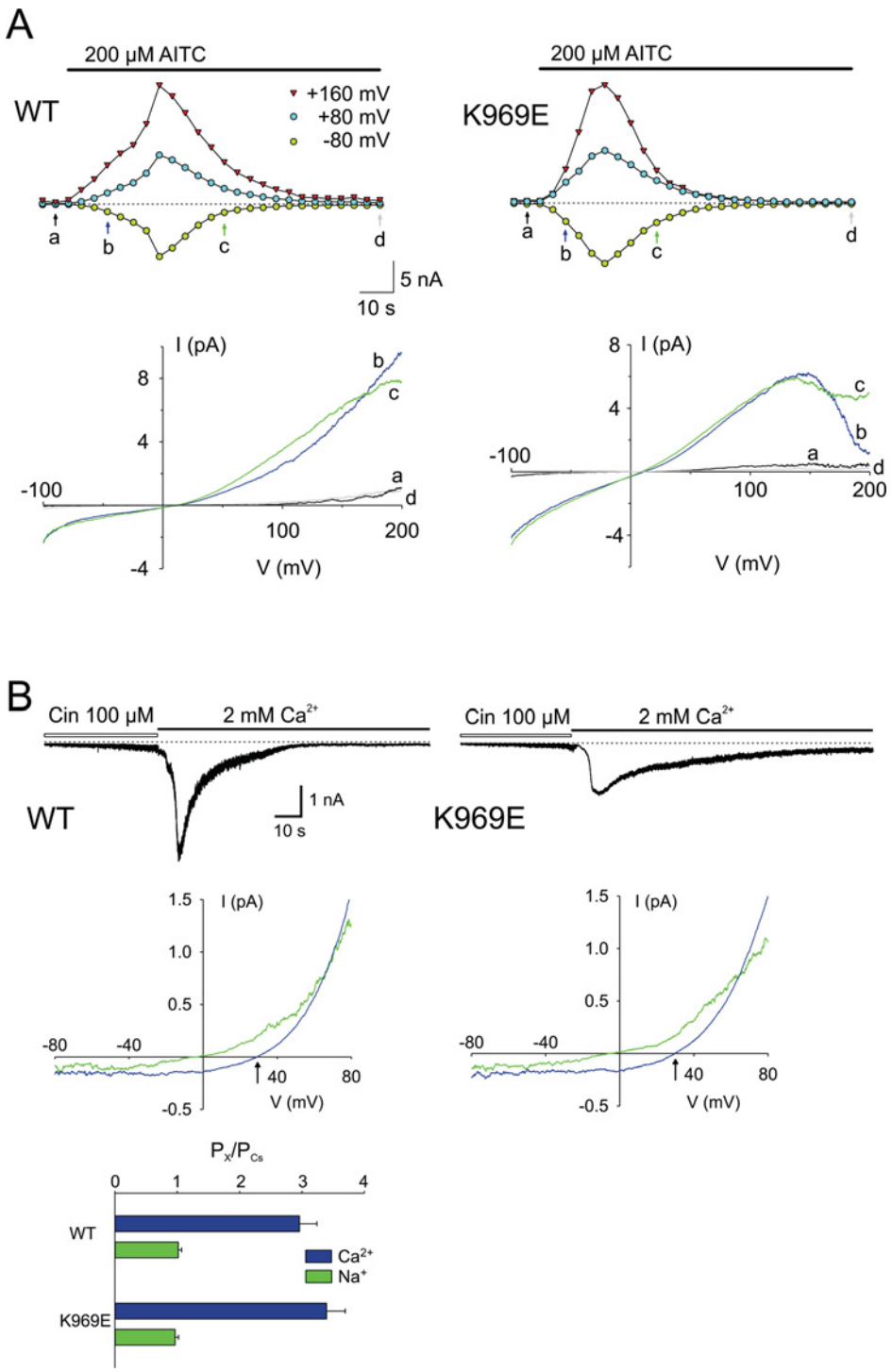

Figure S1 Mutation K969E does not affect the ion permeation properties of TRPA1

(**A**) Effects of the charge-reversing mutation K969E on chemical sensitivity and voltage-dependent properties of the recombinant human TRPA1 channel transiently expressed in HEK-293T cells. The voltage protocol consisted of 600 ms ramps from -100 mV to $+200$ mV applied every 3.8 s, first in extracellular control solution, and then in the maintained presence of 200 μM AITC (bar above the record). Time course of whole-cell membrane currents mediated by wild-type (left) and mutant (right) TRPA1 channel, measured at -80 mV (green circles), $+80$ mV (blue circles) and $+160$ mV (red triangles). Note the changes in the onset of activation in K969E. Voltage ramp traces measured without any stimulation (a), at the onset phase of the AITC response (b), at the inactivation phase (c) and at fully inactivated state of the channels (d). Panels below the time courses are current–voltage relationships of the traces measured at the times indicated by arrows as a, b, c and d above. Currents through K969E decay at more positive membrane potentials (>100 mV). The very close proximity of the first C-terminus helix (comprising Lys^{969}, Arg^{975}, Lys^{988} and Lys^{989}) to the putative inner vestibule of the channel makes it tempting to speculate that this helix can be orientated toward the plane of the membrane and its interface with the cytosol and may constitute a gating ring that transforms AITC-modification energy or depolarization into the mechanical energy necessary to open the pore. (**B**) Ca^{2+} permeability relative to Cs^{+} was measured by using a ramp depolarization (1 V/s) in bi-ionic conditions similar to those described previously [1]. Inward currents were activated by $\sim$40 s exposure to cinnamaldehyde (Cin) and voltage-induced currents were measured first in Ca^{2+}-free bath solution and then in high Ca^{2+} bath solution (128 mM Ca^{2+}). In agreement with published data [2,3], wild-type (WT) TRPA1 channels exhibited relative permeability P_{Ca}/P_{Cs} of 3.0 ± 0.2 ($n = 7$). The K969E mutation yielded channels with unchanged permeability to Ca^{2+} ($P_{Ca}/P_{Cs} = 3.4 \pm 0.3$; $P < 0.05$; $n = 6$), which indicates that this mutation does not affect the ion

permeation process and most likely does not indirectly influence the Ca^{2+}-dependent gating of the channel. The Ca^{2+}-free bath solution contained 150 mM NaCl, 10 mM Hepes and 2 mM EDTA, pH 7.3. For ion-permeability experiments, the high Ca^{2+} bath solution contained 128 mM $CaCl_2$ and 10 mM Hepes (pH 7.3 with NaOH) and the pipette solution contained 5 mM EGTA, 3 mM $CaCl_2$ (100 nM free Ca^{2+}), 145 mM CsCl, 2 mM MgATP and 10 mM Hepes, pH 7.3 with CsOH. Cinnamaldehyde solution was prepared from a 0.1 M stock solution in DMSO so that the final concentration of DMSO in the solutions applied to cells was 0.1 %. The relative permeability P_{Ca}/P_{Cs} was calculated based on the reversal potential (V_{rev}) of the currents measured first in Ca^{2+}-free bath solution and then in the high Ca^{2+} bath solution (with Ca^{2+} as the only permeant ion) according to the rearranged constant-field equation $P_{Ca}/P_{Cs} = ([Cs^+]_i/4 \cdot [Ca^{2+}]_o) \exp(V_{rev}F/RT) [\exp(V_{rev}F/RT)+1]$, where F is Faraday's constant, R is the gas constant and T is temperature [4]. The permeability ratio P_{Na}/P_{Cs} was calculated according to the equation $P_{Na}/P_{Cs} = \exp(V_{rev}F/RT)$. The reversal potential was corrected for the liquid junction potential (in the range 2–5 mV).

REFERENCES

1 Wang, Y. Y., Chang, R. B., Waters, H. N., McKemy, D. D. and Liman, E. R. (2008) The nociceptor ion channel TRPA1 is potentiated and inactivated by permeating calcium ions. J. Biol. Chem. **283**, 32691–32703

2 Ding, S. and Horn, R. (2003) Effect of S6 tail mutations on charge movement in Shaker potassium channels. Biophys. J. **84**, 295–305

3 Benedikt, J., Samad, A., Ettrich, R., Teisinger, J. and Vlachova, V. (2009) Essential role for the putative S6 inner pore region in the activation gating of the human TRPA1 channel. Biochim. Biophys. Acta **1793**, 1279–1288

4 Owsianik, G., Talavera, K., Voets, T. and Nilius, B. (2006) Permeation and selectivity of TRP channels. Annu. Rev. Physiol. **68**, 685–717

Received 10 August 2010/28 September 2010; accepted 14 October 2010
Published as BJ Immediate Publication 14 October 2010, doi:10.1042/BJ20101256